49th AIAA Aerospace Sciences Meeting including the New Horizons Forum and Aerospace Exposi
4 - 7 January 2011, Orlando, Florida
AIAA 2011-46

High-Order Methods for Diffusion Equation with Energy Stable Flux Reconstruction Scheme

K. Ou*, P. Vincent†, and A. Jameson ‡

Aeronautics and Astronautics Department, Stanford University, Stanford, CA 94305

This study investigates the viscous term formulation for the newly developed energy stable flux reconstruction (ESFR) scheme, as an extension to the linear advection flux formulation in the original ESFR scheme. The concept of energy stability for the flux reconstruction approach is put forward. This paper also discusses the formulation of inviscid first derivative flux based on flux reconstruction and diffusive second derivative flux based on solution reconstruction. Numerical experiments for the linear advection equation, diffusion equation, advection-diffusion equation and viscous Burger's equations are performed. The stability and accuracy of three recovered schemes, i.e. Nodal Discontinuous Galerkin, Spectral Difference, and Huynh type methods, are studied. Lastly, the choice and implementation of the interface numerical flux are found to affect the stability and accuracy of the various schemes. In particular, central flux is compared with the unbiased upwind and downwind flux.

I. Introduction

Traditional CFD methods are in general second order accurate schemes. In contrast are high order methods that can achieve arbitrary order of accuracy and produce significant less numerical dissipation than low-order methods. On the other hand, traditional low order schemes are very robust and very simple to implement. They have also been extensively tested and validated in industry. High order methods are in general more complex and less robust. Making the current high order methods simpler, more robust, and more stable is an area of active research. In recent work by Vincent, Castonguay and Jameson,[1] a new class of high-order energy stable flux reconstruction schemes has been developed for linear advection equation. As suggested by its name, this new class of flux reconstruction scheme is energy stable. Various high order methods can be recovered by changing a single parameter in the scheme. This new approach has the potential to offer robustness, efficiency, simplicity and unification to various high order schemes, hence a step towards the goal of wide-spread adoption of high order schemes. In this study, we extend the energy stable flux reconstruction scheme to deal with the viscous term by considering the diffusion equation.

The rest of the paper is organized as follows. We first discuss the concept of energy stability, and present a brief overview of the energy stability estimate for various high order methods such as nodal Discontinuous Galerkin[2–5] and Spectral Difference.[6–10] In parallel, we outline the the Flux Reconstruction scheme proposed by Huynh[11] and analyze the energy stability estimate for Flux Reconstruction scheme. These set the theme for a short overview of the Energy Stable Flux Reconstruction Scheme in the following section. In greater details, we then present the formulation for the viscous term within the Energy Stable Flux Reconstruction Scheme. This is followed by numerical tests to validate current implementation.

II. Brief Overview of Energy Stablility and Flux Reconstruction Scheme

Here we sketch the overall ideas behind the energy estimate of high order methods and the flux reconstruction scheme. The details of each can be found in Hesthaven,[13] Jameson[14] and Huynh[11] respectively.

*PhD Candidate, Aeronautics and Astronautics Department, Stanford University, AIAA Student Member.
†Post Doc, Aeronautics and Astronautics Department, Stanford University.
‡Thomas V Jones Professor, Aeronautics and Astronautics Department, Stanford University, AIAA Fellow.

Here we consider the linear advection equation:

$$\frac{\partial u}{\partial t} + a\frac{\partial u}{\partial x} = 0$$

Consider the energy estimate for the linear advection by multiplying the linear advection equation by u and integrate over the domain x that spans [a,b],

$$\int_a^b u\left(\frac{\partial u}{\partial t} + a\frac{\partial u}{\partial x}\right)dx = 0$$

which, after expansion, shows it satisfies the energy estimate,

$$\frac{d}{dt}\int_a^b \frac{u^2}{2}dx = \frac{1}{2}a(u_a^2 - u_b^2)$$

II.A. Energy Stability Proof for NDG

The following note outlines the proof of the stability of the DG method for 1D linear advection equation in an energy norm of

$$||u|| = \int \left(\frac{u^2}{2}\right)dx$$

Nodal DG Discretization for Linear Advection

As a first step, we derive the nodal DG discretization for the linear advection equation in strong form. In nodal DG, linear advection is discretized by introducing collocation points x_j in each element and define the local solution by the Lagrange polynomial of degree $p = n - 1$.

$$u_h^k = \sum_{j=1}^{n} u_j l_j(x)$$

where u_h^k is the discrete solution in element k. For convenience, the elements have been transformed to reference elements covering the interval [-1,1]. At the same time, the discrete residual in the element k is written as

$$R_h^k = \frac{\partial u_h^k}{\partial t} + \frac{\partial f(u_h^k)}{\partial x}$$

The Galerkin method requires the residual of the equation to be orthogonal to the basis functions. The strong form for the nodal Galerkin can be obtained by firstly integrating by parts to obtain the weak form, and then integrating the middle term of the weak form back by parts. The final result is

$$\int_{-1}^{1} \frac{\partial u_h^k}{\partial t} l_j dx + \int_{-1}^{1} l_j \frac{\partial f(u_h^k)}{\partial x}dx + [\hat{f} - f(u_h^k)]l_j\Big|_{-1}^{1} = 0$$

where $\hat{f}$ is the numerical flux at the element interface. The same equation can be cast in a matrix form by defining the reference mass and stiffness matrices

$$\mathbf{M^k}\frac{d\mathbf{u}}{dt} + \mathbf{S^k f} + \mathbf{l}(\hat{f} - f)\Big|_{x_L}^{x_R} = 0 \quad where \quad \mathbf{M^k}_{ij} = \int_{-1}^{1} \frac{(x_R - x_L)}{2} l_i l_j dx \quad and \quad \mathbf{S^k}_{ij} = \int_{-1}^{1} l_i l_j' dx$$

For the purpose of better illustrating the SD and Flux Reconstruction energy stability proof in the later part of the paper, we can follow the flux reconstruction pocedure proposed by Huynh and rewrite the flux at each boundary as

$$\hat{f}(-1) = au_h(-1) + f_{CL}, \qquad \hat{f}(1) = au_h(1) + f_{CR}$$

where f_{CL} and f_{CR} are boundary corrections

$$f_{CL} = \hat{f}(-1) - au_h(-1), \qquad f_{CR} = \hat{f}(1) - au_h(1)$$

With these, and for simplicity assuming upwind flux so there is no correction on the right, the strong form of the nodal DG scheme can alternatively be expressed as

$$\mathbf{M^k}\frac{d\mathbf{u}}{dt} + \mathbf{S^k f} - f_{CL}l(x_L) = 0$$

Energy Stability Proof for Nodal DG

In Hesthaven,[13] the stability of the nodal discontinuous Galerkin method has been proved for the linear advection equation, by showing that the solution discretized by nodal DG satisfies a similar estimate as the continuous linear advection, shown previously. The proof is sketched as follows. Taking the strong form of the discretized linear advection equation, and multiply it with the local solution to obtain

$$\mathbf{u}^T\mathbf{M}^k\frac{d\mathbf{u}}{dt} + \mathbf{u}^T\mathbf{S}^\mathbf{k}\mathbf{f} + \mathbf{u}^T\mathbf{l}(\hat{f} - f)\Big|_{x_L}^{x_R} = 0$$

Since M^k and S^k have been pre-integrated exactly, this is equivalent to

$$\frac{d}{dt}\int_{x_L}^{x_R}\frac{u_h^2}{2}dx + a\int_{x_L}^{x_R}u_h\frac{\partial u_h}{\partial x}dx + u_h(\hat{f} - au_h)\Big|_{x_L}^{x_R} = 0$$

Here the middle term can be integrated and combined with the last term

$$\frac{d}{dt}\int_{x_L}^{x_R}\frac{u_h^2}{2}dx = -(u_h\hat{f} - a\frac{u_h^2}{2})\Big|_{x_L}^{x_R}$$

In order to establish the DG scheme to be energy stable, the term to the right of the equal sign needs to have negative contributions except at the boundary inputs. It has been shown that there is a negative contribution at every element boundary except the inflow boundary, which is strictly less than the true boundary contribution, hence completing the proof that the DG scheme is energy stable for the linear advection equation.

II.B. Energy Stability Proof for SD

Analysis in this section outlines the proof of the stability of the SD method. Because of the difference between the SD method and the nodal DG method, the proof that the SD method is stable for 1D linear advection equation for all orders of accuracy is established in an energy norm of the Sobolev type instead. Specifically using solution polynomial of degree p, which are expected to yield accuracy of order $p+1$. The norm is

$$||u|| = \int\left(u^2 + c\left(\frac{\partial^p u}{\partial x^p}\right)^2\right)dx$$

where the coefficient c will be discussed later.

Spectral Difference Discretization for Linear Advection

Like the nodal DG scheme, in the SD scheme the discrete solution is locally represented by Lagrange polynomial on the solution collocation points x_j as

$$u_h = \sum_{j=1}^{n} u_j l_j(x)$$

where for polynomials of degree p, $n = p+1$. u_h is the discrete solution in a reference element spanning [-1,1]. However, unlike the nodal DG scheme, the flux is represented by a separate Lagrange polynomial, $\hat{l}_j(x)$, of degree $p+1$, defined by the $n+1$ flux collocation points $\hat{x}_j$

$$f_h = \sum_{j=1}^{n+1} f_j\hat{l}_j(x)$$

For this discrete flux, the interior values at the flux collocation points f_j are set equal to $f(u_h(\hat{x}_j))$ where $u_h(\hat{x}_j)$ is interpolated from $u_h(x)$. At the element boundaries $f(-1)$ and $f(1)$ are defined to be the single valued numerical flux $\hat{f}$. Again follow the flux reconstruction procedure proposed by Huynh and rewrite

the boundary flux in terms of boundary corrections f_{CL} and f_{CR}, the discrete flux can be expanded and rewritten as

$$f_h(x) = f_{CL}\hat{l}_1(x) + \sum_{j=1}^{n+1} f_j \hat{l}_j(x) + f_{CR}\hat{l}_{n+1}(x)$$

For linear advection $f = au$, and also since $au_h(x)$ is a polynomial of degree p, it is exactly represented by the sum in the middle term. Hence

$$f_h(x) = f_{CL}\hat{l}_1(x) + au_h(x) + f_{CR}\hat{l}_{n+1}(x)$$

Finally by differentiating the flux polynomial at the solution collocation we arrive at the SD scheme as

$$\frac{\partial u_h}{\partial t} + \left[a\frac{\partial u_h(x)}{\partial x} + f_{CL}\hat{l}'_1(x) + f_{CR}\hat{l}'_{n+1}(x) \right] = 0$$

To show more clearly the similarity and difference between the nodal DG and SD schemes, we go a step further and cast the SD scheme in matrix form. Evaluting the SD scheme at the solution points we have

$$\frac{du_i}{dt} + \left[a\sum_{j=1}^{n} \mathbf{D}_{ij}u_j + f_{CL}\frac{d\hat{l}_1}{dx}(x_i) + f_{CR}\frac{d\hat{l}_{n+1}}{dx}(x_i) \right] = 0, \quad where \;\; \mathbf{D} = \mathbf{M^{-1}S}$$

To convert the SD scheme to a form that resembles the nodal DG method, we multiply the equation by the mass matrix, and also assuming upwind flux like before so now f_{CR} is equal to zero, to get

$$\sum_j \mathbf{M_{ij}}\frac{du_i}{dt} + a\sum_{j=1}^{n} \mathbf{S}_{ij}u_j + f_{CL}\sum_j \mathbf{M_{ij}}\hat{l}'_1(x_i) = 0$$

Expanding the mass matrix in the last term, this can be further reduced to

$$\sum_j \mathbf{M_{ij}}\frac{du_i}{dt} + a\sum_{j=1}^{n} \mathbf{S}_{ij}u_j - f_{CL}l_i(-1) = f_{CL}\int_{-1}^{1} l'_i(x)\hat{l}_1(x)dx$$

We see that the SD scheme differs from the DG scheme only by the right hand side term!

Energy Stability Proof for SD

To prove the energy stability of the SD scheme, it is most effective to consider an approach that can best leverage the nodal DG stability proof presented earlier. To achieve this, it is desirable to eliminate the difference between the nodal DG scheme and the SD scheme, as shown in the previous section, while at the same time retain the basic form of the two schemes. To this end, a new matrix $\mathbf{Q}$ is proposed in place of the mass matrix $\mathbf{M}$ so that its introduction leads the SD scheme to the following form,

$$\sum_j \mathbf{Q_{ij}}\frac{du_i}{dt} + a\sum_{j=1}^{n} \mathbf{S}_{ij}u_j - f_{CL}l_i(-1) = 0$$

If a suitable $\mathbf{Q}$ can be identified as above so that the basic form is retained while the term that differentiates DG and SD is removed or absorbed, we can attain an energy estimate for the SD scheme with the norm $\mathbf{u^T Q u}$ replacing the norm $\mathbf{u^T M u}$ in the nodal DG scheme in each element. The requirements for $\mathbf{Q}$ can be summarized as follows,

1. It has the following form $\mathbf{Q} = \mathbf{M} + \mathbf{C}$
2. It retains the function of the mass matrix and satisfies $\mathbf{QD} = \mathbf{S}$
3. The last two requirements lead to the third requirement that $\mathbf{CD} = \mathbf{0}$
4. The expansion of the follwing term eliminates the term that differentiates the SD and DG schemes such that $f_{CL}\sum_j \mathbf{Q_{ij}}\hat{l}'_1(x_i) = f_{CL}l_i(-1)$

It is shown by Jameson[14] that the above requirements can indeed be satisfied by choosing the matrix

$$\mathbf{Q} = \mathbf{M} + cdd^T$$

where d^T is the p^{th} difference operator. The first, second and third requirements are satisfied, since for any polynomial $R_p(x)$ of degree p, the combined operation by d and $\mathbf{D}$ on $R_p(x)$ leads to $(p+1)^{th}$ derivative on p^{th} degree polynomial, which is zero.

$$\sum_j d_i \sum_j D_{ij} R_p(x_j) = R_p^{p+1} = 0$$

This leaves only the parameter c to be determined which can satisfy the last requirement. It is shown that this is possible by picking c as

$$c = \frac{2p}{2p+1} \frac{1}{c_p^2} \frac{1}{p!(p+1)!} > 0$$

where $c_p = \frac{1 \cdot 3 \cdot 5 \ldots (2p-1)}{p!}$ is the leading coefficients of the Legendre polynomial $L_p(x)$ of degree p.

So finally, with this choice of $\mathbf{C} = cdd^T$ and $\mathbf{Q} = \mathbf{M} + \mathbf{C}$, the SD scheme can be written in the following form,

$$\sum_j \mathbf{Q_{ij}} \frac{du_i}{dt} + a \sum_{j=1}^{n} \mathbf{S}_{ij} u_j - f_{CL} l_i(-1) = 0$$

and now the same argument that was used to prove the energy stability of the nodal DG shceme establishes the energy stability of the SD scheme with the norm

$$||u|| = \int \left(u^2 + c \left(\frac{\partial^p u}{\partial x^p} \right)^2 \right) dx$$

for the case of solution polynomial of degree p, provided the interior flux collocation points are the zeros of the Legendre polynomial $L_p(x)$.

II.C. Energy Stability Proof for FR

Flux Reconstruction Scheme for Linear Advection

The flux reconstruction scheme was proposed by Huynh.[11] The details of the scheme can be found in the accompaning reference. For completeness, the essential ideas of flux reconstruction are outlined here. Like the previous two schemes, the discrete solution is locally represented by Lagrange polynomial on the solution collocation points x_j as

$$u_h = \sum_{j=1}^{n} u_j l_j(x)$$

where for polynomials of degree p, $n = p + 1$, and u_h is the discrete solution in a reference element covering $[-1, 1]$. However, the representation of the discrete flux with the current approach is different. The discrete flux $f_j(x)$ is required to be continuous across elements. In one hand, it should take on the single valued numerical fluxes at the element interfaces, while on the other it should represent the interior discrete solutions as much as possible.

In the FR scheme, the continous $f_j(x)$ is now made up of an interior flux term f_j^D and a correction flux term f_j^C. The interior flux represents the constructed flux using the discrete solution at the interior of the element. Its interpolated values at the element interfaces are in general discontinuous, hence we label this discrete flux f_h^D, and it is written as

$$f_h^D = \sum_{j=1}^{n+1} f_j^D l_j(x)$$

For this discrete flux, the interior values at the solution collocation points f_j^D are set equal to $f^D(u_h(x_j))$ where $u_h(x_j)$ is the discrete solution at the solution collocation points x_j. The discrete flux at the element interfaces $f_h^D(-1)$ and $f_h^D(1)$ are the interpolated values from $f_h^D(x)$, and, in general, are discontinous across the interfaces.

While f_h^D best represents the interior solutions, at the element interface it differs from the desired continuous flux f_j by, taking the left boundary as an example,

$$f_h^C(-1) = f_{CL} = f_h(-1) - f_h^D(-1) = \hat{f}(-1) - f_h^D(-1)$$

The introduction of the correction flux f_j^C aims to enforce the numerical flux, and hence continuity, at the element boundaries, while trying to minimize the difference between f_h and f_h^D in the interior of the element. In order to define a f^C with such properties, consider a degree $k+1$ correction function $g_L = g_L(r)$ and $g_R = g_R(r)$ that approximate zero (in some sense) within the element while satisfying

$$g_L(-1) = 1, \quad g_L(1) = 0 \quad \& \quad g_R(-1) = 0, \quad g_R(1) = 1$$

A suitable expression for f^C can now be written in terms of g_L and g_R as

$$f_h^C = f_{CL}\ g_L + f_{CR}\ g_R$$

The discrete flux f_h that has continuous values across the element can now be constructed as follows

$$f_h = f_h^D + f_h^C$$

Finally we differentiate the flux at the solution collocation points to obtain

$$\frac{du_i}{dt} + \left[\sum_{j=1}^{n+1} f_j^D \frac{dl_j}{dx}(x_i) + f_{CL}\frac{dg_L}{dx}(x_i) + f_{CR}\frac{dg_R}{dx}(x_i) \right] = 0$$

or for linear advection with $f = au$, this can be written as

$$\frac{du_i}{dt} + \left[a\sum_{j=1}^{n+1} u_j \frac{dl_j}{dx}(x_i) + f_{CL}\frac{dg_L}{dx}(x_i) + f_{CR}\frac{dg_R}{dx}(x_i) \right] = 0$$

This final form of the Flux Reconstruction scheme also quite closely resembles the form of the SD scheme shown previously.

Energy Stability Proof for FR

From the earlier section, we derived the energy estimate for the SD scheme using boundary flux corrections in a way very similar to the Flux Reconstruction scheme. The connection between the two schemes are (to some degree) implied by the similarity of the final forms of the schemes. Hence it is also plausible to approach the energy estimate of the FR scheme using a similar norm of the form

$$||u|| = \int u^2 + c_0 \left(\frac{\partial^p u}{\partial x^p} \right)^2 dx$$

where c_0 for FR scheme is to be determined.

Starting with the FR scheme, we can derive the explicit expressions for the two terms that make up the norm. The results are quoted below, while details can be found in Vincent, Castonguay and Jameson (2010). For the first term,

$$\frac{d}{dt}\int_{-1}^{1} u_j^2 dx = -\hat{a}[u_R^2 - u_L^2] - 2f_{CL}\left(-u_L - \int_{-1}^{1} g_L \frac{\partial u_h}{\partial x} dx \right) - 2f_{CR}\left(u_R - \int_{-1}^{1} g_R \frac{\partial u_h}{\partial x} dx \right)$$

and for the second term, setting $c_0 = \frac{c}{2}$,

$$\frac{1}{2}\frac{d}{dt}\int_{-1}^{1} c\left(\frac{\partial^p u_h}{\partial x^p} \right)^2 dx = -2cf_{CL}\left(\frac{\partial^p u_h}{\partial x^p} \right)\left(\frac{d^{p+1} g_L}{dx^{p+1}} \right) - 2cf_{CR}\left(\frac{\partial^p u_h}{\partial x^p} \right)\left(\frac{d^{p+1} g_R}{dx^{p+1}} \right)$$

and lastly adding the two equations together we obtain the desired explicit expression as

$$\begin{aligned}\frac{d}{dt}\int_{-1}^{1} u_j^2 + \frac{c}{2}\left(\frac{\partial^p u_j}{\partial x^p}\right)^2 dx = &+ 2(f_{CL}u_L - \hat{a}\frac{u_L^2}{2}) - 2(f_{CR}u_R - \hat{a}\frac{u_R^2}{2}) \\ &+ 2f_{CL}\left[\int_{-1}^{1} g_L \frac{\partial u_h}{\partial x}dx - c\left(\frac{\partial^p u_h}{\partial x^p}\right)\left(\frac{d^{p+1}g_L}{dx^{p+1}}\right)\right] \\ &+ 2f_{CR}\left[\int_{-1}^{1} g_R \frac{\partial u_h}{\partial x}dx - c\left(\frac{\partial^p u_h}{\partial x^p}\right)\left(\frac{d^{p+1}g_R}{dx^{p+1}}\right)\right]\end{aligned}$$

If the last two terms of the above equation are set equal to zero, from the section where energy stability of DG scheme is presented, we see that we recover the same form of the DG scheme. This is also the similar approach used to prove SD scheme energy stability. From the previous section, the energy estimate for the SD scheme depends on the choice of the parameter c. Hence we expect the same for the FR scheme. Vincent, Castonguay and Jameson[1] shows that provided the following three conditions are met,

1. Condition a: $\int_{-1}^{1} g_L \frac{\partial u_h}{\partial x}dx - c\left(\frac{\partial^p u_h}{\partial x^p}\right)\left(\frac{d^{p+1}g_L}{dx^{p+1}}\right) = 0$
2. Condition b: $\int_{-1}^{1} g_R \frac{\partial u_h}{\partial x}dx - c\left(\frac{\partial^p u_h}{\partial x^p}\right)\left(\frac{d^{p+1}g_R}{dx^{p+1}}\right) = 0$
3. Condition c: $c_0(k) < c < \infty, \quad$ where $c_0(k) = \frac{-2}{(2k+1)(a_k k!)^2}$

the Flux Reconstruction scheme will be energy stable. Since both g_L and g_R are functions of c, the single parameter c determines the stability as well as the type of Flux Reconstruction scheme. The method to determine g_L, g_R, and c such that the above conditons are satisfied is presented in the next section.

III. Brief Overview of Energy Stable Flux Reconstruction Scheme

The Energy Stable Flux Reconstruction scheme follows immediately from the final result of the last section, i.e. any correction functions g_L and g_R with a value of c which meet the energy stability requirements can be used to construct energy stable FR schemes. In this section, we identify the form of flux correction function g_L and g_R, and the parameter c that determines the type of the scheme.

III.A. Flux Correction Function

Starting with the conditions that will lead to energy stability for the FR scheme, and due to symmetry, consider only the one related to the left flux correction function,

$$\int_{-1}^{1} g_L \frac{\partial u_h}{\partial x}dx - c\left(\frac{\partial^p u_h}{\partial x^p}\right)\left(\frac{d^{p+1}g_L}{dx^{p+1}}\right) = 0$$

This expression is dependent of the flow solution. Substituting $u_h = \sum_{j=1}^{n} u_j l_j(x)$ into the equation, we have

$$\sum_{j=1}^{n+1} u_j \left[\int_{-1}^{1} g_L \frac{\partial l_j}{\partial x}dx - c\left(\frac{\partial^p l_j}{\partial x^p}\right)\left(\frac{d^{p+1}g_L}{dx^{p+1}}\right)\right] = 0$$

which can be satisfied independently of the solution if we can meet the following condition for every j

$$\int_{-1}^{1} g_L \frac{\partial l_j}{\partial x}dx - c\left(\frac{\partial^p l_j}{\partial x^p}\right)\left(\frac{d^{p+1}g_L}{dx^{p+1}}\right) = 0$$

This expression is now dependent of the solution basis through l_j and dependent of the flux correction basis embeded in g_L.

Solution Basis Expansion

The solution basis l_j is a polynomial of degree p, which can be written in the most general form as

$$l_j = a_0 + a_1 x + a_2 x^2 + a_3 x^3 + ... + a_p x^p = \sum_{i=0}^{p} a_i x^i$$

Hence the p^{th} derivative of the solution basis is a constant, which can be found to be the leading coefficient in the expansion of the solution basis. The first derivative of the solution basis can also be found using the expansion of the solution basis. Explicitly, we have for every j

$$\frac{\partial^p l_j}{\partial x^p} = p! a_p \quad , \quad \frac{\partial l_j}{\partial x} = 0 + a_1 + 2a_2 x + 3a_3 x^2 + ... + p a_p x^{p-1} = \sum_{i=1}^{p} i a_i x^{i-1}$$

Substitution back to get, for every j

$$\sum_{i=0}^{p} i a_i \int_{-1}^{1} g_L x^{i-1} dx - c\ p!\ a_p \left(\frac{d^{p+1} g_L}{dx^{p+1}} \right) = 0$$

Flux Correction Function Basis Expansion

Consider expanding g_L in terms of the Legendre polynomials L with the highest degree being $p+1$. The $(p+1)^{th}$ derivative of g_L is a constant. They are written as follows

$$g_L = \sum_{i=0}^{p+1} \phi_i L_i \ \ \& \ \ \frac{d^{p+1} g_L}{dx^{p+1}} = (p+1)! \phi_{p+1}$$

where ϕ_i are the expansion coefficients. Again back substitution leads to

$$\sum_{i=0}^{p} \int_{-1}^{1} \underbrace{\phi_i\ L_i}_{flux} \underbrace{i\ a_i\ x^{i-1}}_{solution} dx - c\ p!\ a_p (p+1)!\ \phi_{p+1} = 0$$

where the contributions from the flux correction basis and the solution basis are explicitly labeled in the equation. The equation can be satisfied independent of the solution basis if $\phi_i = 0$ for $0 \le i \le p-1$, leaving only the last term to make the above equation valid,

$$\underbrace{\sum_{i=0}^{p-1} \int_{-1}^{1} \underbrace{\phi_i\ L_i}_{flux} \underbrace{i\ a_i\ x^{i-1}}_{solution} dx}_{=0 \text{ if } \phi_i = 0 \text{ for } 0 \le i \le p-1} + \int_{-1}^{1} \phi_{p-1}\ L_{p-1}\ p\ a_p\ x^{p-1} dx - c\ p!\ a_p (p+1)!\ \phi_{p+1} = 0$$

Therefore, to fully determine g_L, it only remains to find ϕ_{p-1}, ϕ_p, and ϕ_{p+1}. These can be found by solving the following three equations

1. Energy Stability $\int_{-1}^{1} \phi_{p-1}\ L_{p-1}\ p\ a_p\ x^{p-1} dx - c\ p!\ a_p (p+1)!\ \phi_{p+1} = 0$
2. Left End Point $\phi_{p-1} - \phi_p + \phi_{p+1} = (-1)^{k+1}$
3. Right End Point $\phi_{p-1} + \phi_p + \phi_{p+1} = 0$

These three equations can be solved and the final expressions for the left and right flux correction functions in terms of Legendre polynomials are written as

$$g_L = \frac{(-1)^k}{2} \left[L_k - \left(\frac{\eta_k L_{k-1} + L_{k+1}}{1+\eta_k} \right) \right]$$

$$g_R = \frac{(+1)^k}{2} \left[L_k + \left(\frac{\eta_k L_{k-1} + L_{k+1}}{1+\eta_k} \right) \right]$$

where $\eta_k = \frac{c(2k+1)(a_k k!)^2}{2}$. Use of these correction functions leads to energy stable FR schemes with a suitable c. The choices of c that lead various schemes are discussed in the next section.

III.B. Example of Energy Stable FR Schemes

Nodal DG scheme

By the choice of c, if the flux correction functions are reduced to the right and left Radau polynomials, then a nodal scheme is recovered. The corresponding flux correction functions are

$$g_L = \frac{(-1)^k}{2}(L_k - L_{k+1})$$

$$g_R = \frac{(+1)^k}{2}(L_k - L_{k+1})$$

which is a result of picking $c = 0$.

SD scheme

The SD scheme has a set of flux collocation points within the element. At those points, the flux correction functions should assume zero values. By choosing $c = \frac{2k}{(2k+1)(k+1)(a_k k!)^2}$, the resulting flux correction functions are

$$g_L = \frac{(-1)^k}{2}(1 - x)L_k$$

$$g_R = \frac{(+1)^k}{2}(1 + x)L_k$$

Huynh Type scheme

If the value of c is set equal to $\frac{2(k+1)}{(2k+1)k(a_k k!)^2}$, the resulting flux correction functions are

$$g_L = \frac{(-1)^k}{2}\left[L_k - (\frac{(k+1)L_{k-1} + kL_{k+1}}{2k+1})\right]$$

$$g_R = \frac{(+1)^k}{2}\left[L_k + (\frac{(k+1)L_{k-1} + kL_{k+1}}{2k+1})\right]$$

This recovers a particular scheme that was proposed by Huynh, which was found to be very stable.

IV. Energy Stable Flux Reconstruction Scheme for Diffusion Equation

Consider the general scalar conservation law with both the convection term and diffusion term

$$\frac{\partial u}{\partial t} + \frac{\partial}{\partial x}f^i(u) + \frac{\partial}{\partial x}f^v(u_x) = 0$$

for which the linear convection flux is $f^i(u) = au$, where a is the advection wave speed. The diffusive flux is $f^v(u_x) = -\mu\frac{\partial u}{\partial x}$, where μ is the diffusion coefficient. The linear advection term has been solved using the flux reconstruction scheme by Huynh (2007), and later in the context of energy stable flux reconstruction scheme by Vincent, Castonguay and Jameson (2010). The reconstruction approach was used again by Huynh (2009)[12] for solving diffusion equation. Here we employ the similar simple and efficient formulation for the diffusive term in the context of energy stable flux reconstruction scheme.

IV.A. Solution Reconstruction

Restrict our attention to the diffusion equation,

$$\frac{\partial u}{\partial t} + \frac{\partial}{\partial x}f^v(u_x) = \frac{\partial u}{\partial t} - \frac{\partial}{\partial x}(\mu\frac{\partial u}{\partial x}) = 0$$

which is discretized by representing the discrete solution u_h in each element as an expansion in a set of Lagrange basis defined at solution collocation points within the transformed element covering $[-1, 1]$. For

diffusion equation, both the first and the second solution derivatives need to be evaluated. This requires the solution to be continuous across the element interface. In the FR scheme, the continuous u_h is now made up of a piecewise discontinuous interior solution polynomial u_h^D and a solution correction polynomial u_h^C that corrects the discontinuous solutions at the interface to a common value, hence enforcing continuity at the element boundaries .

Interior Solution Representation

The interior discrete solution u_h^D in each element is represented as an expansion in a set of Lagrange basis defined at solution collocation points within the element.

$$u_h^D = \sum_{j=1}^{n} u_j^D l_j(x)$$

The solutions at the element boundaries $u_h^D(-1)$ and $u_h^D(1)$ are the interpolated values from u_h^D.

Single Valued Interface Solution

At the element interface, the solution values to the left and right of the interface in general have different values. A single valued interface value $\hat{u}$ need to be assumed, which is common to the element and its left or right neighbor. This can be chosen to be one sided value so that it takes either the solution to the left or to the right of the interface, or it can be the average value. Since diffusion problem has no directional preference, the central value is used. Now the difference between the interpolated solution at the element boundary $u_h^D(-1)$ or $u_h^D(1)$, and the single valued interface solution $\hat{u}(-1)$ or $\hat{u}(1)$ can be written as boundary corrections,

$$u_{CL} = \hat{u}(-1) - u_h^D(-1), \quad u_{CR} = \hat{u}(1) - u_h^D(1)$$

Solution Correction Representation

The solution correction function u_h^{CL} is a polynomial that, when superimposed on u_h^D, corrects $u_h^D(-1)$ to the single valued $\hat{u}(-1)$ at the element left boundary while minimizing any contribution to u_h^D at the element interior. A suitable function is a polynomial g_L that approximates zero function while satisfying the following boundary conditions

$$g_L(-1) = 1, \quad g_L(1) = 0$$

Similarly a right solution correction functionu_h^{CR} can be defined with

$$g_R(1) = 1, \quad g_R(-1) = 0$$

A further requirement for g_L and g_R are that they are degree $p+1$ polynomials. This allows their derivatives to be of the same degree order as the solution polynomial. The left and right solution correction functions are written as

$$u_h^{CL} = u_{CL} g_L, \quad u_h^{CR} = u_{CR} g_R$$

Reconstructed Continuous Solution Representation

Finally, the reconstructed solution that is continuous across the element interface can be written as follows, expressed as the superposition of the discrete interior solution and the solution correction polynomials,

$$u_h = u_h^D + u_h^C, \quad with \quad u_h^C = u_h^{CL} + u_h^{CR}$$

IV.B. First Solution Derivative

Finally we differentiate the reconstructed solution at the solution collocation points to obtain

$$\frac{\partial u}{\partial x}(x_i) = \sum_{j=1}^{n+1} u_j^D \frac{dl_j}{dx}(x_i) + u_{CL}\frac{dg_L}{dx}(x_i) + u_{CR}\frac{dg_R}{dx}(x_i)$$

To make the analysis for the second solution derivative easier, we define a new parameter v to present the first solution derivative such that at each solution collocation points

$$v_i = \frac{\partial u}{\partial x}(x_i)$$

IV.C. Diffusive Flux Reconstruction

With the first solution derivative set equal to v, the evaluation of the second solution derivative follows the standard flux reconstruction method with the flux now being the diffusive flux. Diffusive flux is set equal to $f^v = -\mu v$. As before, discrete f_h^v is represented by the discontinuous interior part ${f^v}_h^D$ and the interface flux correction part ${f^v}_h^C$.

$$f_h^v = {f^v}_h^D + {f^v}_h^C$$

Interior Diffusive Flux Representation

Firstly, with the usual notations defined previously, express the discrete representation of v_h^D within the interior of the element as

$$v_h^D = \sum_{j=1}^{n} v_j^D l_j(x)$$

The diffusive flux is also expressed by Lagrane polynomial on the corresponding solution collocation points as

$${f^v}_h^D = \sum_{j=1}^{n} {f^v}_j^D l_j(x)$$

The element boundary values are interpolated from ${f^v}_h^D$ to get the left boundary flux ${f^v}_h^D(-1)$ and the right boundary flux ${f^v}_h^D(1)$ respectively.

Interface Numerical Diffusive Flux

At the boundary interface, the single valued numerical diffusive flux can again be chosen as one sided or central type. Since the interface solution was previously taken as the average of the values to the left and right of the interface, the same central type is used here. If a one-sided approach is used previously, then the preference should be given to the opposite side here to cancel any direction bias to best reflect the diffusion process. We label the numerical diffusive flux $\hat{f}^v$. The diffusive flux correction at the boundaries are

$${f^v}_{CL} = \hat{f}^v - {f^v}_h^D(-1) \quad and \quad {f^v}_{CR} = \hat{f}^v - {f^v}_h^D(1)$$

Diffusive Flux Correction Function

The same polynomial that approximates zero function is used to correct the left and right boundary flux. Scale the left and right boundary values to the appropriate diffusive flux correction values to arrive at the left and right diffusive flux correction functions

$${f^v}_h^C = f_{CL}^v \; g_L + f_{CR}^v \; g_R$$

Reconstructed Diffusive Flux

The discrete diffusive flux f_h^v that has continuous values across the element can now be constructed as follows

$$f_h^v = {f^v}_h^D + {f^v}_h^C$$

IV.D. Diffusive Flux Divergence

Finally we differentiate the diffusive flux at the solution collocation points to obtain

$$\frac{du_i}{dt} + \left[\sum_{j=1}^{n+1} {f^v}_j^D \frac{dl_j}{dx}(x_i) + f_{CL}^v \frac{dg_L}{dx}(x_i) + f_{CR}^v \frac{dg_R}{dx}(x_i) \right] = 0$$

V. Numerical Results

In this section, the energy stable flux reconstruction schemes have been applied to solve a range of model equations including the linear advection equation, diffusion equation, advection-diffusion equation, and viscous Burger's equation. Extension of the current scheme to 2D quadrilateral mesh is straightforward using tensor product approach, while actual implementation is work in progress. The following 1D results demonstrate the flexibility and capability of the current scheme to solve a range of problems including those with viscosity and non-linearity. The ease of switching between various recovered schemes also allows us to quickly assess the characteristics of different methods. In particular, we evaluate the performance of the nodal DG, SD and Huynh type methods. The choice of numerical flux and its impact of stability and accuracy are also investigated. All the computations are integrated in time using the explicit five-stage fourth order TVD Runge-Kutta method.

V.A. Results for Linear Advection Equation

The linear advection problem was presented in the work of Vincent, Castonguay and Jameson.[1] It is presented here for completeness. Consider the governing equation for the linear advection:

$$\frac{du}{dt} + c\frac{\partial u}{\partial x} = 0 \tag{1}$$

One exact solution is:

$$u = -e^{-20(x-ct)^2}$$

with period boundary condition and the following initial solution

$$u = -e^{-20x^2}.$$

The computational domain covers [-1,1], with a total of 10 equal sized mesh elements. 3^{rd} order schemes are used in all cases. The advection speed is set to $c = 1$. The equation is solved to a final time of $T = 20s$ with a fixed time step of $dt = 0.04s$. The numerical flux is chosen as upwind flux. Table 1 summarizes the

c=1,T=20s, 10 Mesh Elements Between [-1,1]			
Scheme	dt	Numerical Flux Type	L^2 norm error
NDG	0.04	Upwind	0.052499706677135
SD	0.04	Upwind	0.137380796178796
HU	0.04	Upwind	0.184285792871284

Table 1. L^2 norm error at T=20s

L^2 norm errors of the NDG, SD and Huynh schemes at T=20s, while figure 1 plots the final solutions at T=20s. From both the table and the plots of final solutions, we can see that DG scheme produces the most accurate result. This is followed by SD scheme and then Huynh scheme.

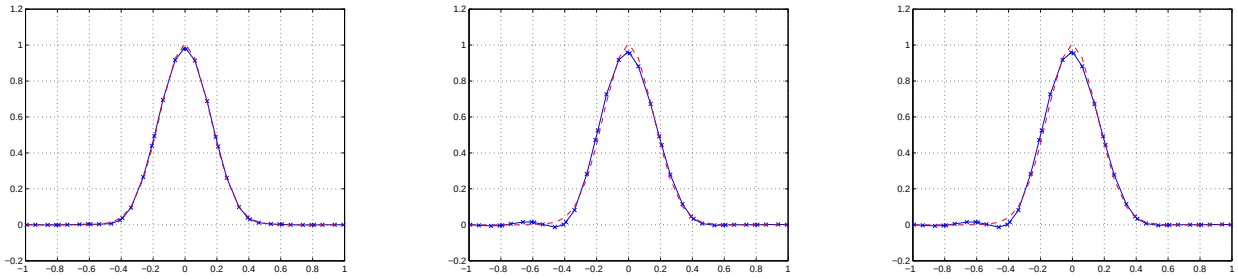

(a) DG (b) SD (c) HU

Figure 1. High Order Schemes for Advection Equation with Flux Reconstruction at t=20s

V.B. Results for Diffusion Equation

Consider the following governing equation for diffusion:

$$\frac{du}{dt} - \mu \frac{\partial^2 u}{\partial x^2} = 0 \tag{2}$$

One exact solution is:

$$u = \sqrt{\frac{t_0}{t}} e^{\frac{-x^2}{4\mu t}}$$

with the boundary conditions:

$$u = \sqrt{\frac{t_0}{t}} e^{\frac{-{x_0}^2}{4\mu t_0}}$$

and the initial solution:

$$u = e^{\frac{-x^2}{4\mu t_0}}$$

The computational domain has the left and right boundaries located at -3 and 3 respectively, with a total of 30 equally spaced elements. The coefficient of diffusion is set equal to $\mu = 0.01$. The time constant is chosen to be $t_0 = 1$. In all cases, the 4^{th} order schemes are used. The computation starts at $t = t_0$ and terminates at $T = 20s$. Table 2 (a)-(c) summarized the L^2 norm errors for computations with decreasing time step. The interface numerical flux for the first derivative is chosen as upwind flux. The interface numerical flux for the second derivative is chosen as the downwind flux. The results indicate that nodal DG requires smaller time step than the other two schemes to remain stable. However, DG also produces results with least error for a stable time step. In summary, DG is the most accurate but least stable (in terms of time step requirement) while Huynh type method is the most stable but least accurate.

Scheme	dt	Interface Flux (1^{st} Derivative/2^{nd} Derivative)	L^2 norm errors
NDG	0.07	Upwind/Downwind	not converged
SD	0.07	Upwind/Downwind	not converged
HU	0.07	Upwind/Downwind	2.658075009941668e-05

(a)

Scheme	dt	Interface Flux (1^{st} Derivative/2^{nd} Derivative)	L^2 norm errors
NDG	0.06	Upwind/Downwind	not converged
SD	0.06	Upwind/Downwind	1.917712068468873e-05
HU	0.06	Upwind/Downwind	2.658075080075107e-05

(b)

Scheme	dt	Interface Flux (1^{st} Derivative/2^{nd} Derivative)	L^2 norm errors
NDG	0.04	Upwind/Downwind	1.056750184880397e-05
SD	0.04	Upwind/Downwind	1.917712146335072e-05
HU	0.04	Upwind/Downwind	2.658075159798373e-05

(c)

Table 2. L^2 norm error at T=20s with unbiased upwind/downwind flux

To study the effect of choosing different numerical flux, the same computations are performed with central flux for both the first and second derivatives. The results are tabulated in table 3. In table 3 (a), the same time step as table 2 (c) is used. Comparing the results from these two tables, we find that upwind flux leads to results with smaller error for all schemes. On the other hand, the central scheme allows all the methods to have larger time step without going unstable, as indicated by table 3 (b).

The final solutions at time $T = 20s$ are plotted in figure 2. All the solutions agree well with the exact solution (in red).

Scheme	dt	Interface Flux (1^{st} Derivative/2^{nd} Derivative)	L^2 norm errors
NDG	0.04	Central/Central	2.488340951088608e-05
SD	0.04	Central/Central	3.943743226435352e-05
HU	0.04	Central/Central	4.912928200061465e-05

(a)

Scheme	dt	Interface Flux (1^{st} Derivative/2^{nd} Derivative)	L^2 norm errors
NDG	0.1	Central/Central	2.488341096546930e-05
SD	0.1	Central/Central	3.943743342646491e-05
HU	0.1	Central/Central	4.912928307300747e-05

(b)

Table 3. L^2 norm error at T=20s with central flux

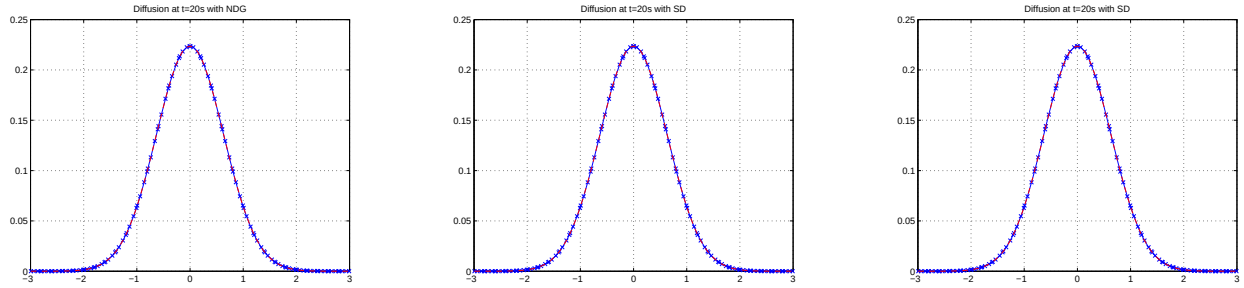

(a) DG (b) SD (c) HU

Figure 2. High Order Schemes for Diffusion Equation with Flux Reconstruction at t=20s

V.C. Results for Advection and Diffusion

Consider the governing equation for advection and diffusion:

$$\frac{du}{dt} + c\frac{\partial u}{\partial x} - \mu\frac{\partial^2 u}{\partial x^2} = 0 \tag{3}$$

One exact solution is:

$$u = \sqrt{\frac{t_0}{t}} e^{\frac{-x^2}{4\mu t}} - e^{-20(x-ct)^2}$$

with the boundary conditions:

$$u = \sqrt{\frac{t_0}{t}} e^{\frac{-{x_0}^2}{4\mu t_0}}$$

and the initial solution:

$$u = e^{\frac{-x^2}{4\mu t_0}} - e^{-20x^2}$$

The computation domain is made of 30 equally spaced elements between -3 to 3. The advection speed is $c = 1$, the diffusion coefficient is $\mu = 0.01$, and the time constant is $t_0 = 1$. In all cases, 4^{th} order schemes have been used. The computation is run to a final time $T = 18s$ for different time steps and the results are summarized in table 4 (a)-(c). The results are consistent with the previous observations of the different schemes' stability and accuracy. Schemes with increasing accuracy are Huynh type, SD, and nodal DG, while schemes with increasing stability are nodal DG, SD, and Huynh type method. The final solutions are plotted in figure 3. Again, very good agreement with the exact solution is found for all cases. The 4^{th} order scheme produces far less numerical dissipation compared to the 3^{rd} order advection case. The oscillations that are present in the 3^{rd} order case are not observed here. It will be interesting to see if the presence of diffusion term helps smoothing the oscillations when recompute the current case with 3^{rd} order schemes.

Scheme	dt	Numerical Flux(1^{st} Derivative/2^{nd} Derivative)	L^2 norm errors
NDG	0.05	Upwind/Downwind	not converged
SD	0.05	Upwind/Downwind	not converged
HU	0.05	Upwind/Downwind	5.440331255639303e-05

(a)

Scheme	dt	Numerical Flux(1^{st} Derivative/2^{nd} Derivative)	L^2 norm errors
NDG	0.04	Upwind/Downwind	not converged
SD	0.04	Upwind/Downwind	3.022895070940816e-05
HU	0.04	Upwind/Downwind	4.149456163554698e-05

(b)

Scheme	dt	Numerical Flux(1^{st} Derivative/2^{nd} Derivative)	L^2 norm errors
NDG	0.02	Upwind/Downwind	1.192204072425836e-05
SD	0.02	Upwind/Downwind	2.485778675435708e-05
HU	0.02	Upwind/Downwind	3.602209833027569e-05

(c)

Table 4. L^2 norm error at T=18s

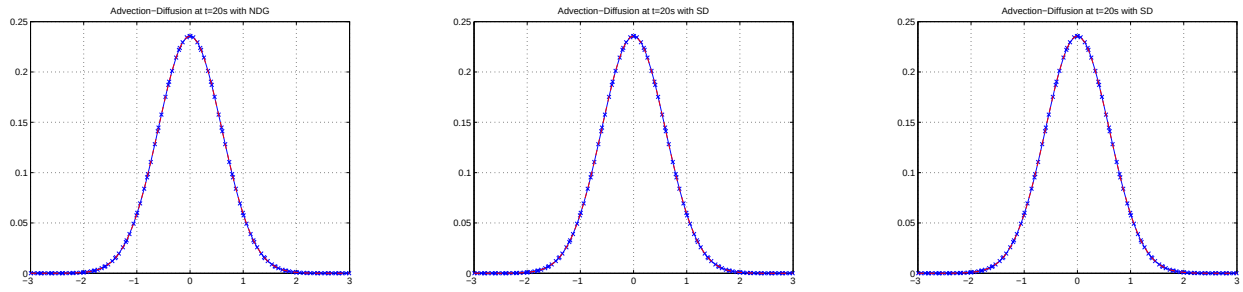

(a) DG (b) SD (c) HU

Figure 3. High Order Schemes for Advection-Diffusion Equation with Flux Reconstruction at t=18s

V.D. Results for Viscous Burger's

Finally consider the governing equation for the non-linear viscous Burger's:

$$\frac{du}{dt} + u\frac{\partial u}{\partial x} - \mu\frac{\partial^2 u}{\partial x^2} = 0 \tag{4}$$

One exact solution is:

$$u = 0.5\left[1 - tanh(\frac{x - t/2}{4\mu})\right]$$

with the boundary conditions:

$$u_l = 0.5\left[1 - tanh(\frac{x_l - t/2}{4\mu})\right]$$

$$u_r = 0.5\left[1 - tanh(\frac{x_r - t/2}{4\mu})\right]$$

and the initial solution:

$$u_0 = 0.5\left[1 - tanh(\frac{x_0}{4\mu})\right]$$

In the computational domain spanning -2 and 2, a total of 40 equally spaced mesh elements are used. The 4^{th} order schemes are used. The viscous coefficient is set equal to $\mu = 0.02$. The steep gradient centers at $x = 0$ at $t = 0$. At time t, the center position of the steep slope is located at $x = \frac{t}{2}$. The computation terminates at $T = 0.5s$. The final solutions are plotted in figure 4. The L^2 norm errors are tabulated in table 5. The central flux is used for both the first and second derivatives of the viscous term. For the non-linear convection term, upwind flux is used. These results are shown in table 5 (a) - (c) with decreasing time step. In table 5 (d), the unbiased upwind-downwind fluxes are used for the viscous term.

Scheme	dt	Numerical Flux (1^{st} and 2^{nd} Viscous Derivative/Burger's)	L^2 norm errors
NDG	0.018	Central - Central/Upwind	not converged
SD	0.018	Central - Central/Upwind	not converged
HU	0.018	Central - Central/Upwind	0.002523898726280

(a)

Scheme	dt	Numerical Flux (1^{st} and 2^{nd} Viscous Derivative/Burger's)	L^2 norm errors
NDG	0.016	Central - Central/Upwind	not converged
SD	0.016	Central - Central/Upwind	0.002239539772574
HU	0.016	Central - Central/Upwind	0.002522978418570

(b)

Scheme	dt	Numerical Flux (1^{st} and 2^{nd} Viscous Derivative/Burger's)	L^2 norm errors
NDG	0.009	Central - Central/Upwind	0.001846295504394
SD	0.009	Central - Central/Upwind	0.002240483727267
HU	0.009	Central - Central/Upwind	0.002522780905728

(c)

Scheme	dt	Numerical Flux (1^{st} and 2^{nd} Viscous Derivative/Burger's)	L^2 norm errors
NDG	0.005	Upwind - Downwind/Upwind	0.001197812199523
SD	0.005	Upwind - Downwind/Upwind	0.001726730194813
HU	0.005	Upwind - Downwind/Upwind	0.002497489706339

(d)

Table 5. L^2 norm error at T=0.5s

As before, we find that central flux allows larger time steps than unbiased upwind/downwind flux, but is less accurate. Scheme with increasing accuracy are Huynh, SD, and DG methods, while scheme with increasing stability are DG, SD and Huynh methods.

VI. Error Convergence Study

In this final section, we summarize the previous numerical results in the form of error convergence study. We show that the current formulation for the diffusion term produces solutions with convergence characteristics expected of this class of methods. We also compare the error convergence for various recovered schemes to illustrate the findings we discussed in the previous section. Solutions to the viscous Burger's equation are also considered. The error convergence for the non-linear viscous model equation also behaves as expected.

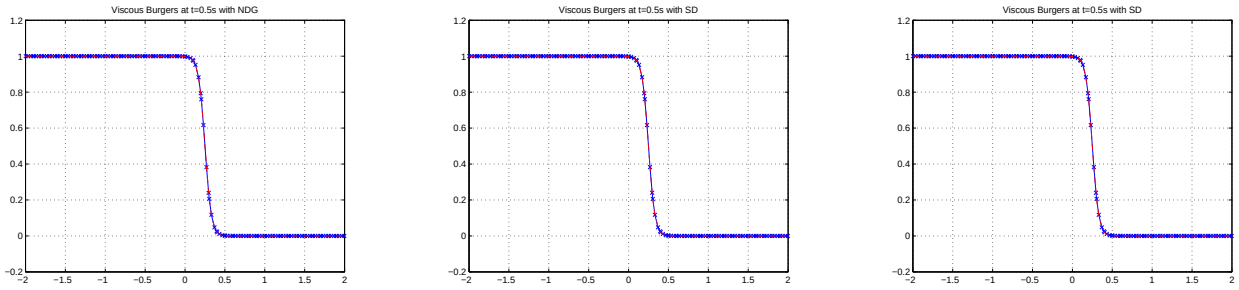

(a) DG (b) SD (c) HU

Figure 4. High Order Schemes for Viscous Burger's Equation with Flux Reconstruction at t=0.5s

VI.A. Error Convergence for Diffusion Equation

Diffusion equation is solved with the ESFR schemes. Three recovered schemes, ie. nodal DG, SD, and Huynh type, have been used. The diffusion equation is advanced to a final time t=10s with $\mu = 0.01$. Central flux is used as the Riemann flux for the first and the second derivative term. The 3rd, 4th and 5th order results are plotted in figure 5 for all three schemes.

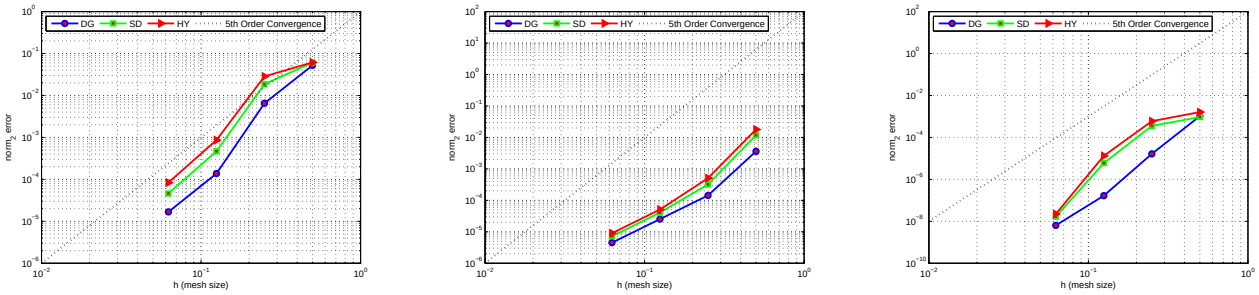

(a) 3rd order result (b) 4th order result (c) 5th order result

Figure 5. Error convergences for diffusion equation solved with the 3rd, 4th and 5th order ESFR schemes. Recovered schemes include nodal DG, SD, and Huynh schemes.

It is seen from the figure that, with the solution reconstruction approach for the 2nd derivative diffusive term in the diffusion equation, all three methods based on the ESFR schemes produce the right orders of accuracy. We also observe that the recovered nodal DG scheme produces the least error with the strictest time step restriction. Huynh scheme has more error but allows larger time step. SD scheme acts as a good compromise of these two schemes.

VI.B. Error Convergence for Viscous Burger's Equation

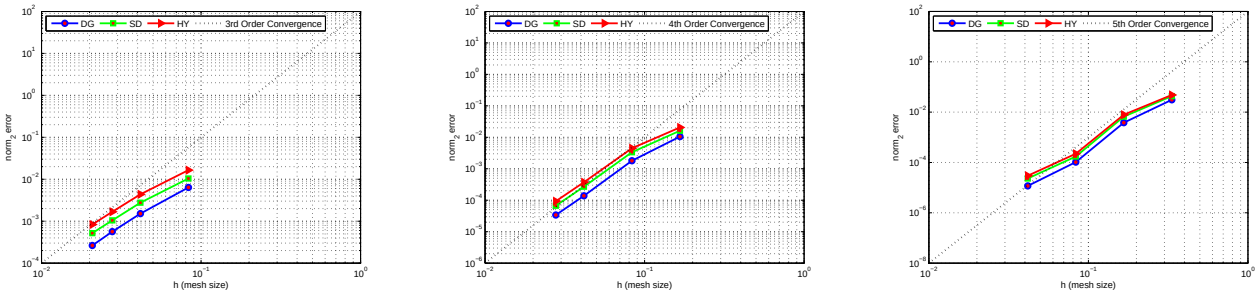

(a) 3rd order result (b) 4th order result (c) 5th order result

Figure 6. Error convergences for viscous Burger's equation solved with the 3rd, 4th and 5th order ESFR schemes.

To show that the ESFR scheme works well not only for the linear and diffusive equations, but also for the

general non-linear viscous equation, the error convergences for the solutions to the viscous Burger's equation are presented in figure 6. The viscous Burger's equation is advanced to a final time t=4s with $\mu = 0.02$. Upwind flux is used as the Riemann flux for the convective term, while upwind and downwind fluxes are used for the first and the second derivative term respectively. In all the three cases considered, expected orders of convergence are obtained.

VII. Conclusion

In the first part of this study, the energy stability approach for proving and constructing high order schemes is reviewed. In particular, the high order spectral difference scheme has been proved to be stable using this approach. The flux reconstruction scheme proposed by Huynh was analyzed with the energy stability framework, and new energy stable schemes emerge from this framework. In the second part of this study, we present the solution reconstruction approach for the viscous flux for the energy stable flux reconstruction scheme. This formulation is tested with a range of model equations in 1D, including the diffusion equation, advection-diffusion equation, and non-linear viscous Burger's equation. We compared three typical schemes recovered from the energy stable flux reconstruction scheme, and found that nodal DG is the most accurate scheme of the three, but has the most stringent time step requirement. In the contrast, the Huynh type scheme allows the largest time step but has the largest error. The Spectral Difference method has characteristics that are in between nodal DG and Huynh scheme. Lastly, the impact of interface flux choice on stability and accuracy is briefly investigated. The central flux is found to be more stable than upwind flux, but at the expense of reduced accuracy. Overall, this study combines the previous work[1] on linear advection, which uses flux reconstruction approach for the 1st derivative inviscid flux term, with the viscous flux formulation based on solution reconstruction approach for the 2nd derivative diffusive term, and demonstrates through various numerical tests the flexibility and capability of the new energy stable flux reconstruction scheme. The current method can be extended to multi-dimensions in 2D quadrilateral and 3D hex meshes with tensor-product approach in a straightforward manner. Extension to triangular and tetrahedra meshes are more challenging, but is currently work in progress. While the simple formulation for the viscous term works well, there is still room to explore for potentially more efficient and accurate formulations. This is also an area under study. Nevertheless, this work lays the foundation for the future development of a high order Navier-Stokes solver based on the energy stable flux reconstruction concept.

Acknowledgement

This research work is made possible by the generous support from the National Science Foundation and the Air Force Office of Scientific Research under the grants 0708071 and 0915006 monitored by Dr. Leland Jameson, and grant FA9550-07-1-095 by Dr. Fariba Fahroo. The authors would like to thank them for their continuous support.

References

[1]P. Vincent, P. Castonguay and A. Jameson, *A New Class of High-Order Energy Stable Flux Reconstruction Schemes*, J. Sci. Comput. (2010).

[2]B. Cockburn and C. Shu, *Runge–Kutta Discontinuous Galerkin Methods for Convection-Dominated Problems*, J. Sci. Comput. **16**, 173 (2001).

[3]D. N. Arnold, F. Brezzi, B. Cockburn, and L. D. Marini, *Unified analysis of discontinuous Galerkin methods for elliptic problems*, SIAM J. Numer. Anal. **39**, 1749 (2001).

[4]J. S. Hesthaven and T. Warburton, *Nodal high-order methods on unstructured grids*, J. Comput. Phys. **181**, 186 (2002).

[5]F. X. Giraldo, J. S. Hesthaven, and T. Warburton, *Nodal high-order discontinuous Galerkin methods for the spherical shallow water equations*, J. Comput. Phys. **181**, 499 (2002).

[6]D. A. Kopriva and J. H. Kolias, *A conservative staggered-grid Chebyshev multidomain method for compressible flows*, J. Comput. Phys. **125**, 244 (1996).

[7]Y. Liu, M. Vinokur, and Z. J. Wang, *Spectral difference method for unstructured grids I: basic formulation*, J. Comput. Phys. **216**, 780 (2006).

[8]Z. J. Wang, Y. Liu, G. May, and A. Jameson, *Spectral difference method for unstructured grids II: extension to the Euler equations*, J. Sci. Comput. **32**, 45 (2007).

[9]Y. Liu, M. Vinokur, and Z. J. Wang, *High-Order Multidomain Spectral Difference Method for the Navier-Stokes Equations on Unstructured Hexahedral Grids*, Communications in Computational Physics **Vol 2**, Number 2, pp 310-333 (2006).

[10]C. Liang, A. Jameson, and Z. J. Wang, *Spectral difference method for compressible flow on unstructured grids with mixed elements*, J. Comput. Phys. **228**, 2847 (2009).

[11]H. T. Huynh, *A flux reconstruction approach to high-order schemes including discontinuous Galerkin methods*, Number AIAA-2007-4079, AIAA Computational Fluid Dynamics Conference, 2007.

[12]H. T. Huynh, *A Reconstruction Approach to High-Order Schemnes Including Discontinuous Galerkin for Diffusion* , 47th AIAA Aerospace Sciences Meeting including The New Horizons Forum and Aerospace Exposition, Orlando, Florida, Jan. 5-8, 2009

[13]J. S. Hesthaven and T. Warburton, *Nodal discontinuous Galerkin methods - Algorithms, analysis, and applications*, Springer, (2008).

[14]A. Jameson, *A proof of the stability of the spectral difference method for all orders of accuracy*, J. Sci. Comput. (2010).